An Evaluation of the JPL TOPSAR for Extracting Tree Heights

Yutaka Kobayashi, Kamal Sarabandi, *Fellow, IEEE*, Leland Pierce, *Member, IEEE*, and M. Craig Dobson

***Abstract*—In this paper, the accuracy of the digital elevation model (DEM) generated by the Jet Propulsion Laboratory (JPL) TOPSAR for extracting canopy height is evaluated. For this purpose, an experiment using C-band TOPSAR at the Michigan Forest Test Site (MFTS) in Michigan's Upper Peninsula was conducted. Nearly 25 forest stands were chosen in MFTS, which included a variety of tree types, tree heights, and densities. For these stands, extensive ground data were also collected. The most important and difficult-to-characterize ground truth parameter was the forest ground level data, which is required for extracting the height of the scattering phase center from the interferometric SAR(INSAR) DEM. To accomplish this, differential global positioning system (GPS) measurements were done to accurately ($\pm$5 cm) characterize the elevation of: 1) a grid of points over the forest floor of each stand and 2) numerous ground control points (GCPs) over unvegetated areas.**

Significant discrepancies between GPS and TOPSAR DEM and between the two TOPSAR DEMs of the same area were observed. The discrepancies are attributed to uncompensated aircraft roll and multipath. An algorithm is developed to remove the residual errors in roll angle using elevation data from: 1) 100-m resolution U.S. Geological Survey DEM and 2) the GPS-measured GCPs. With this algorithm, the uncertainties are reduced to within 3 m. Still, comparison between the corrected TOPSAR DEMs shows an average periodic height discrepancy along the cross-track direction of about $\pm$5 m. Simulation results show that this might have been caused by multipath from an object near one of the INSAR antennas. Careful examination of the coherence image and the backscatter image also show such periodic patterns. Recommendations are provided for the extraction of the best estimate of the scattering phase center height, and a model is provided to estimate actual tree height. It is accurate to within 1 m or 10% for the red pine test stands used here.

***Index Terms*—Calibration, environmental factors, image analysis, interferometry, radar applications, radar data processing, synthetic aperture radar (SAR), vegetation.**

I. Introduction

ONE OF the most critical biophysical parameters that is needed for accurate global climate model (GCM) predictions is biomass. Radar has been used extensively in attempts to estimate this parameter, especially for trees. Previous work of ours has used the strategy of accurately classifying the trees to several structural categories followed by class-specific inversion models for various biomass-related terms [4], [5]. One of the most important of these parameters is the height of the tree canopy. Because synthetic aperture radar (SAR) records both amplitude and phase of the target reflections, two such observations from different locations can be used to infer the elevation of the target. This is called interferometric SAR (INSAR).

Besides the backscattering coefficient image, interferometric SARs provide two additional images that are sensitive to the target parameters. These are the magnitude and phase of the backscatterer cross correlation between the signals received by the two antennas of INSAR. The phase of the interferogram is the quantity from which the height of the pixel (with respect to a reference) is retrieved. The magnitude of the cross correlation, or simply the correlation coefficient, characterizes the uncertainty with which the height can be measured [18]. For random media in which the radar signal can penetrate to some extent such as a vegetation canopy, the measured height is somewhere within the random volume depending on the location and relative strengths of the scatterers comprising the medium. The measured height is the location of the scattering phase center for each pixel which of course is a random variable. The statistics of this scattering phase center height is a function of size, orientation, spatial distribution, and the vertical extent of the random medium. Therefore, the measured scattering phase center height can be used as an independent and sensitive parameter for remote sensing of vegetation.

The coherence was used in an attempt to obtain tree height from repeat-pass ERS-1 data [1], [7]. In those studies, a model was used to predict tree height from the time variation of the coherence. Another study [3] used polarimetric phase differences to obtain images of the phase difference due to the presence of trees but made no attempt to model the actual height, as there was no ground truth.

In an attempt to establish the relationship between the canopy parameters and the INSAR parameters (phase of interferogram and correlation coefficient), simplified theoretical models based on the distorted Born approximation have been developed [17], [18]. These models are first order and are capable of explaining the phenomenology of the problem rather accurately. However, due to their underlying simplifying assumptions, they are not capable of producing very accurate quantitative results. To rectify this deficiency, a sophisticated scattering model based on Monte Carlo simulation of fractal-generated trees was developed recently [14], [15].

For verifying these models and eventually developing an inversion algorithm, experimental data are needed. Since the height of most forest stands range from 10–60 m, accuracy in height measurement of the order of $\pm$0.5 m is needed. Initially, we excluded INSAR data generated by repeat-pass interferometry as the temporal decorrelation and problems with baseline estimation hamper height evaluation with such

Manuscript June 15, 1998; revised February 4, 2000.

The authors are with the Radiation Laboratory, Department of Electrical Engineering and Computer Science, University of Michigan Ann Arbor, MI 48109-2122 USA (e-mail: saraband@eecs.umich.edu).

Publisher Item Identifier S 0196-2892(00)06217-3.

required accuracy. Two-antenna systems such as the JPL TOPSAR are potentially capable of height measurements of the required accuracy.

To examine the feasibility of using INSAR data for estimating tree height, we conducted a set of experiments with Jet Propulsion Laboratory (JPL) TOPSAR over a well-characterized forest test site. The test stands at the Michigan Forest Test Site (MFTS) are chosen to include different tree species at different growth stages and densities. The wealth of data collected at this site over the past several years makes this an ideal area to use. Species composition, diameter, height, and stand densities have been meticulously measured with ground-based tools [2]. Also, much of our previous classification work was done at this test site [6], [8], so we are very familiar with the types and distribution of the vegetation.

This paper is organized as follows: Section II describes the test site and the ground-based measurements. Section III presents the two height estimation algorithms, and Section IV gives the conclusions.

II. Ground Measurements

A. Tree Height Measurements

The MFTS is located in the eastern part of Michigan's Upper Peninsula. The surveyed forest stands cover an area of approximately 20 km $\times$ 20 km, centered at Raco. The species composition, diameters, heights, and number densities were measured over a period of several years ending in 1994 [2]. In some cases, heights of trees were measured with calibrated height poles while in others, heights were estimated based on their diameters and species using equations appropriate to that species under similar growing conditions. Because over 70 000 individual trees were measured in 70 different stands, we feel that the dataset is one of the best available for testing algorithms for tree height estimation.

To supplement this dataset, we wanted closely-spaced and accurate measurements of ground elevation. The data available from the U.S. Geological Survey (USGS) was neither accurate enough nor dense enough (100 m spacing), and so we used differential Global Positioning System (GPS) measurements to obtain our own elevation data.

B. GPS Measurements

GPS consists of many satellites in known orbits that are constantly sending signals to receivers on the ground. The ground receiver uses the known orbits, and the time it takes for each message to propagate from the satellite to triangulate its own position in three dimensions. The accuracy of the measured position increases with more satellites and more messages.

We used the Trimble site surveyor GPS receiver in order to obtain accuracies on the order of 2 cm. This involves the use of a fixed base station and any number of rovers. The base station is a GPS receiver set up over a surveyed benchmark with known three-dimensional (3-D) coordinates. It broadcasts its own signal to the rovers to supplement the satellite signals, and a difference vector is calculated that relates the rover to the base station.

The benchmarks we used were surveyed by the U.S. National Geodetic Survey and are brass plates set in concrete pilings in the ground. The coordinates of these benchmarks can be obtained from NGS at their web site. Note that the coordinates given are referenced to various Earth models called ellipsoids. There are many of these, and it is best to convert from those given to one named WGS-84, as that is the one the GPS receivers use internally. A good review of the ellipsoids used throughout the world is given in Schreier [9].

A typical rover measurement involves

1) setting the antenna on a measured height pole with a level bubble;
2) finding a clear view of the satellites through the trees (the L-band signal is significantly attenuated by even a few branches);
3) initializing so the satellites are tracked and the position fix is within a meter
4) taking a data point by keeping the pole very still and level, waiting for about 10 s for the averaging process to converge to a given error tolerance, usually 2 cm.

There were two kinds of measurements we needed to take with the GPS receivers: 1) ground control points and 2) forest stand floor. The ground control points were specially chosen areas on the ground that we could identify in the SAR images. This usually meant road intersections. These points were needed in order to assure ourselves of the accuracy of the USGS and TOPSAR DEMs. The forest stand floor was measured in order to be able to calculate tree heights above the ground using a simple difference with the TOPSAR DEM. In order to deal with ground height variability in a stand, a grid of points was used. This was the same grid of points used to measure the tree heights originally and consisted of 40 points per 200 m $\times$ 200 m forest stand. The tree stands chosen for this study were monocultures all planted at the same time, resulting in a very uniform height distribution. It took 1–3 h to measure a stand, depending on how often we had to reinitialize because of lost signal from the overlying canopy. In some large, dense stands it was impossible to use the GPS receivers at all, and we contented ourselves with measurements along the stand periphery and field notes about the approximate elevation variation within the stand.

Of course, the USGS and GPS data did not agree exactly. However, the errors were within the expected range given the large (100 m) horizontal spacing of the USGS data.

III. Tree Height Estimation

A. INSAR Overview

In single-pass INSAR, the platform has two antennas as shown in Fig. 1. One antenna transmits and both receive. The path-length differences (δ) between the two signals results in a phase difference (ϕ) given by

$$\phi = \frac{2\pi}{\lambda}\,\delta \tag{1}$$

where λ is the carrier wavelength. Since the geometry of the two antennas is known, the baseline length (B) and the baseline angle (α) can be used to determine the look angle (θ)

$$\sin(\alpha-\theta) = -\frac{(r+\delta)^2 - r^2 - B^2}{2rB} \tag{2}$$

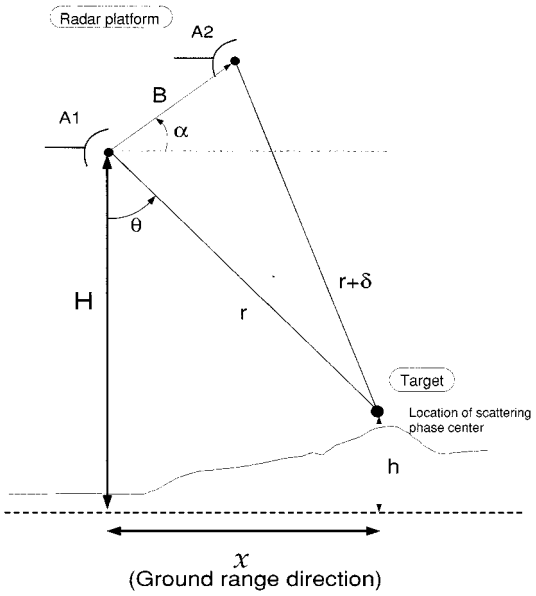

Fig. 1. Geometry of single-pass interferometric SAR (INSAR).

TABLE I
TOPSAR INTERFEROMETRIC PARAMETERS

Parameter	TOPSAR value
Baseline length(B)	2.58meter
Baseline angle(α)	62.77degree
Radar platform height(H)	around 7470meter
Wavelength of carrier frequency(λ)	5.67cm

where r is the range of the target from the transmitting antenna. Using the height of the radar platforms (H) as an arbitrary reference, the target elevation is given by

$$h = H - r\cos\theta. \tag{3}$$

The height h is really the height of the scattering phase center for a given pixel. In the case of trees, the height is somewhere below the height of the top of the canopy. The pertinent parameters for the JPL TOPSAR are given in Table I, while the details concerning the data are given in Table II.

The raw data was processed by JPL into three standard products: 1) C_{vv} power, 2) DEM, and 3) coherence. It is these standard products that are used in this study. Note that the TOPSAR flights occurred in April of 1995 and that the most recent height measurements were taken in the fall of 1994. Since the growing season had not yet started in April, we believe that there was no significant change in the height of the trees during this time.

B. Uncompensated Aircraft Roll Correction

Since the TOPSAR platform [10] is an aircraft, significant effort is expended in measuring and compensating for the deviation of the airplane from smooth level flight. This is called motion compensation and has been successfully applied in the AirSAR data, which uses the same platform but different antennas. Motion compensation must correct for variations from steady, level flight, which includes variations in height, heading, pitch, and roll. As mentioned in [16], the compensation of the roll angle variability is very important, and for TOPSAR, the accuracy of this correction is approximately 0.01°.

In comparing the TOPSAR DEMs of the same area from two different TOPSAR images, we noticed that there was serious disagreement between them. This prompted us to examine the data more carefully. Eventually, we came up with a way of explaining much of the discrepancy with an uncompensated roll angle error of less than 0.3°.

First, we attempted to match the USGS DEM to the TOPSAR DEM, which has an expected height error of about 2 m [11]. This involved converting the USGS DEM into height over the NAD27 ellipsoid and then manually warping it to the TOPSAR image geometry. Residual errors in aircraft altitude and roll angle are lumped into one parameter, namely roll angle error, which is a good approximation for very small values of residual altitude and roll angle errors. The roads and other sparsely vegetated areas were compared as seen in Fig. 2. Apart from a constant difference between the USGS DEM and the TOPSAR DEM, Fig. 2(c) shows a significant variation in the height difference (about 50 m) as a function of along-track distance. This variation far exceeds the expected uncertainties in the TOPSAR and USGS DEMs. We interpreted this as a height error caused by the residual errors in the roll angle. The error in roll angle is directly proportional to the error in the look angle, which is used to calculate the height. Equation (3) can be used to obtain what the height error due to an incorrect look angle would be

$$dh/d\theta = r\sin\theta = x \tag{4}$$

where x is ground range. This shows that the height error is $x\,\Delta\theta$ and so will increase with range and with look-angle error. This is shown in Fig. 2(b) from a given cut along the cross-track direction (about 13 m for 900 pixels). The look angle error can be caused by an uncompensated roll angle error. Unfortunately, a constant roll angle error does not work well for the entire image as can be seen from Fig. 2(c). Hence, we used an azimuth-dependent error model. For each azimuth line, j, we can write

$$\Delta h_j = x\Delta\theta_j + h_{offset} \tag{5}$$

where h_{offset} is some constant height error that can be used to adjust the offset between the TOPSAR and USGS reference planes. In order to use the USGS DEM to correct the TOPSAR DEM, we used only areas in the TOPSAR DEM that were bare spaces or short vegetation. Hence, we classified the images using the C_{vv} power to three classes: bare, short vegetation, and trees. Because we only had one channel, the approach was based on simple thresholds with trees being greater than -15 dB, and bare less than -20 dB.

The error model given by (5) is used in a statistical sense over the entire image. This is done to minimize the error between the USGS and TOPSAR DEMs as the USGS DEM is coarse and has a height uncertainty of approximately ± 3–5 m. Determination of the best value for h_{offset} requires the minimization of the following equation:

$$S = \sum_{i=1}^{M}\sum_{j=1}^{N}(\Delta h_{ij} - x_i\Delta\theta_j - h_{offset})^2 \tag{6}$$

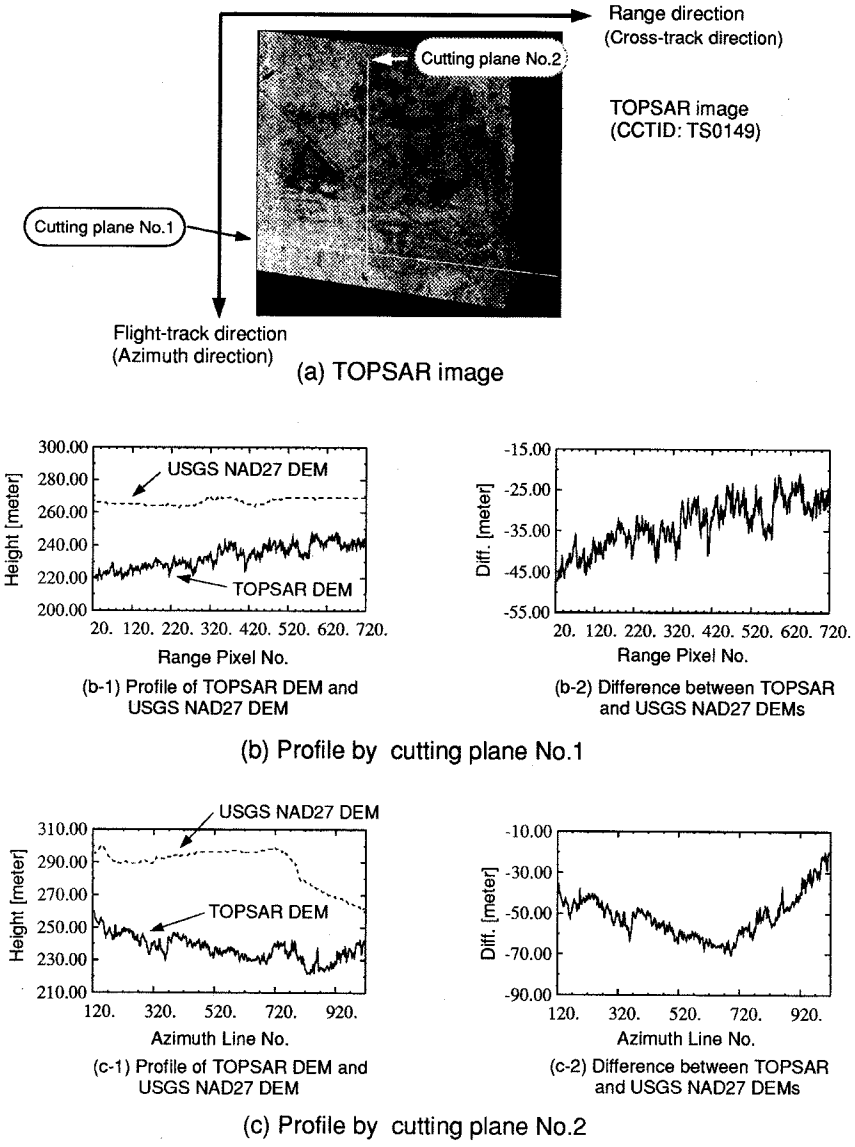

Fig. 2. Comparison between TOPSAR DEM and USGS NAD27 DEM.

TABLE II
DESCRIPTION OF TEST SITE AND DEM DATA FROM THE TOPSAR AND USGS

Michigan Forests Test Site(MFTS)	Located in the eastern part of Michigan's Upper Peninsula. The region is approximately 20 Km square. According to U.S.Geological Survey, the elevation difference in the whole area of MFTS is less than 60 m, which means MFTS is relatively flat area.
TOPSAR DEM	Both ground range and azimuth pixel spacing are 10 m. The following data are used. CCTID:TS0149(Acquired 26-April-1995) CCTID:TS0171(Acquired 26-April-1995) Some regions are covered by both of these two data, but are illuminated at different incidence angles.
USGS DEM	Original pixel spacing is 100 m in both North-South direction and East-West direction. It is interpolated into 10 m spacing. Elevation is based on NAD27 ellipsoid.

where i and j refer to the range and azimuth (along-track) coordinates, respectively, and $\Delta h = h_{\mathrm{TOPSAR}} - h_{\mathrm{USGS}}$. For estimation of h_{offset} (a constant over the entire image), we did not use every azimuth line in the image because the resultant matrix equation was too large. Instead, we subsampled in azimuth, using about 100 lines.

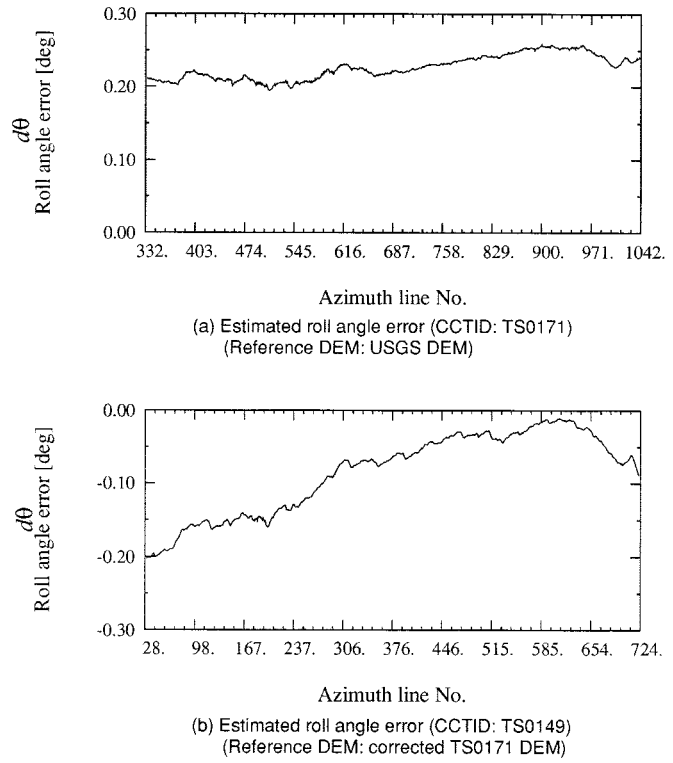

Fig. 3. Estimated roll angle error for two TOPSAR DEMs based on least-square minimization between TOPSAR and USGS data.

The minimization is carried out by finding a stationary point

$$\frac{\partial S}{\partial h_{offset}} = 0, \quad \text{and} \quad \frac{\partial S}{\partial \theta_j} = 0, \qquad \text{for all } j. \tag{7}$$

This results in the following set of equations:

$$h_{offset}MN + \sum_{j=1}^{N}\left(\sum_{i=1}^{M} x_i\right)\Delta\theta_j = \sum_{i=1}^{M}\sum_{j=1}^{N}\Delta h_{ij}$$
$$h_{offset}\left(\sum_{i=1}^{M} x_i\right) + \Delta\theta_j\left(\sum_{i=1}^{M} x_i^2\right) = \sum_{i=1}^{M} x_i \Delta h_{ij}, \qquad \text{for all } j \tag{8}$$

which can be solved for the $\Delta\theta_j$'s and h_{offset}. This h_{offset} is then used for each azimuth line to get $\Delta\theta_j$ using a linear least-squares fit to (5). The resulting roll angle error is a continuous function of azimuth, which makes this believable as an error mechanism, since the airplane cannot have a very high frequency roll angle change. Fig. 3 shows the calculated roll angle error for the two TOPSAR scenes. Note that the error is quite small, less than 0.3° in all cases.

Finally, the calculated height error is compensated for in the TOPSAR DEM pixel-by-pixel. To assess how well we did, we used the ground control points (GCPs) that were collected using GPS. The GCP locations are shown in Fig. 4, and the height errors before and after the roll angle correction are shown in Table III. This shows that the height error has been reduced to an average of about 2 m, although there are still a few points where the error is much worse.

TABLE III
ASSESSMENT OF ROLL ANGLE ERROR COMPENSATION USING GCPS. THE COMPENSATION IMPROVES THE AGREEMENT BETWEEN THE DIFFERENTIAL GPS MEASURED DATA AND TOPSAR DEM. BOTH THE MEAN AND STANDARD DEVIATION OF HEIGHT DIFFERENCE ARE IMPROVED

(a) TOPSAR DEM(CCTID:TS0171, referenced DEM: USGS DEM)

GCP No.	$h_{TOPSAR} - h_{GPS}$ Before compensation	$h_{TOPSAR} - h_{GPS}$ After compensation
1	-54.3	-2.0
2	-43.7	2.2
3	-50.1	-2.7
4	-47.7	-1.8
5	-43.9	0.3
6	-58.7	-3.2
7	-44.8	1.7
8	-68.6	-6.3
Mean	-51.5	-1.5
Standard deviation	8.72	2.82

(b) TOPSAR DEM(CCTID:TS0149, referenced DEM: corrected TS0171 DEM)

GCP No.	$h_{TOPSAR} - h_{GPS}$ Before compensation	$h_{TOPSAR} - h_{GPS}$ After compensation
1	-46.7	-1.4
2	-44.5	-0.5
3	-44.9	-1.7
4	-48.0	-0.6
5	-44.0	-2.0
6	-36.4	-1.3
7	-41.9	-1.8
8	-44.0	-2.4
Mean	-43.8	-1.5
Standard deviation	3.5	0.64

Note that in calculating the TOPSAR DEM height for a given point involves averaging over at least 4×4 pixels in the neighborhood of that point. This is because the phase noise standard deviation is large, and averaging will result in a decreased height error, which in this case is about 3–5 m, comparable to the USGS DEM height errors. This allows comparisons using these heights to be meaningful.

C. Multipath

Despite our efforts in correcting for the roll angle error, there still appear to be some residual errors left. This is most apparent when looking at the C_{vv} power images, as seen in Fig. 5, where a quasiperiodic sinusoid is apparent with the crests parallel to the azimuth direction. The spacing of these crests increases from about 60 pixels in the near range to about 130 in the far range. The same pattern is seen in the DEM data. The magnitude of those errors is approximately 8 dB and 10 m peak-to-peak in the power and elevation images, respectively. This is a significant effect that must be dealt with in order to estimate tree heights accurately. In all fairness, these errors are not present at all with some of the TOPSAR data we have. Unfortunately, for this application this is the only data we could use.

This problem may be due to multipath [12], [13], where an object near the antennas is reflecting the returned pulse into the antennas. The coherent addition of the direct return and the multipath return could cause such a pattern. Assume that the multipath object only reflects into the upper of the two antennas. Also assume that the object is near the upper antenna. These assumptions are made according to the arrangement of the TOPSAR and other AirSAR antennas.

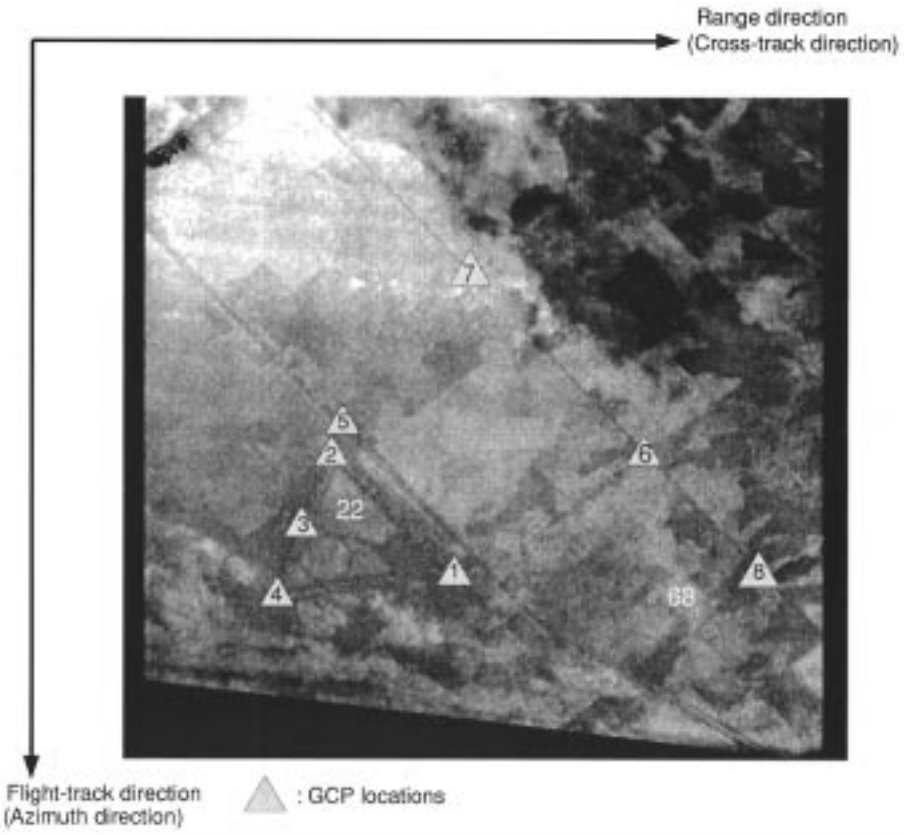

Fig. 4. Corrected TOPSAR DEM(TS0171) showing both the location of the GCPs and the two test forest stands (22 and 68). The DEM image is shown in grey scale such that low to high elevation is shown varying from black to white.

As shown in Fig. 6, we can then model the fields at each antenna as

$$r_{A_1} = E_s e^{ik2A_1T}$$
$$r_{A_2} = E_s[e^{ik(A_1T+A_2T)} + de^{ik(A_1T+TC+CA_2)}] \quad (9)$$

where $k = 2\pi/\lambda$ is the wave number, the terms A_1T, A_2T, TC and CA_2 are the path lengths, and d is a diffraction coefficient. If we represent the additional path length due to the multipath object as $\Delta L = TC + A_2C - A_2T$, we can write the amplitude error as

$$\frac{|r_{A_2}|^2 - |E_s|^2}{|E_s|^2} = d^2 + 2d\cos(k\Delta L) \approx 2d\cos(k\Delta L). \quad (10)$$

It can easily be shown that $(TC - TA_2)$ increases with increasing range in a nonlinear fashion, which gives rise to a sinusoid whose period increases with range. We can also derive an expression for the phase difference that this would induce in the interferogram phase. Representing this error in phase by ϕ_{error} and noting that $d \ll 1$, it can be shown that

$$\phi_{error} = L[e^{ik(A_2T-A_1T)} + de^{ik(TC+CA_2-A_1T)}] - Le^{ik(A_2T-A_1T)} \approx d\sin(k\Delta L). \quad (11)$$

Equations (10) and (11) indicate that the phase and power errors are in phase quadrature.

These equations were used to calculate the expected multipath error, which was compared to the known error. First, the period of the oscillation as a function of range was used to narrow in on the best position for a single scatterer, then the peak-to-peak variation was used to get the best diffraction coefficient. Unfortunately, the best we could do with a single scatterer did not match the range varying period exactly, and so there remained residual errors. The result was unsatisfactory.

This led us to try another approach. Apparently, the TOPSAR processing involves a step where a measured phase screen is applied to the data in order to remove any multipath that is repeatable. This phase screen is calculated by JPL at the beginning of each deployment season and depends on a very accurate DEM, that is compared with the TOPSAR data to produce the phase error as a function of the look angle. We obtained a copy of this phase screen and used it as in the multipath equations above in order to correct both the DEM and power data from TOPSAR. Unfortunately, the variations due to this correction still did not exactly cancel the variations in the data we had, and so this method did not work either.

Consequently, we gave up in our attempt to correct for the multipath error. Unfortunately, this limited the number of forest test stands we could use, since only a few had bare spots near them that were unaffected by the multipath errors.

D. Tree Height Estimation

The corrected DEM is now as consistent with the USGS DEM and the GCPs collected with GPS as was possible. The determination of the height of the trees is next. While the C-band, vv-polarized signal scatters significantly from branches and needles or leaves in the crown, the scattering phase center is rarely at the top of the trees, so we need a model that relates it to the true

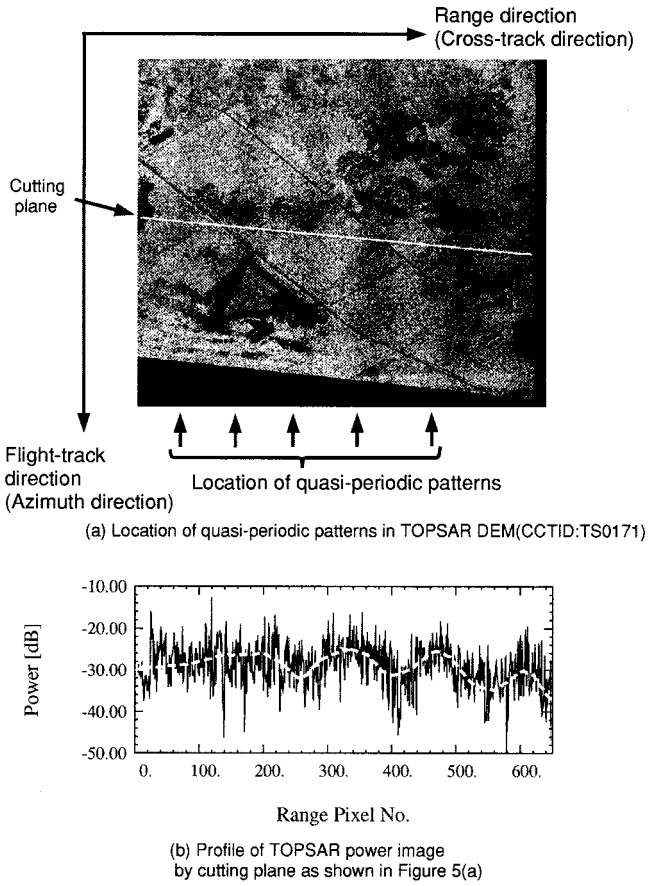

Fig. 5. Location of quasiperiodic patterns in TOPSAR power image

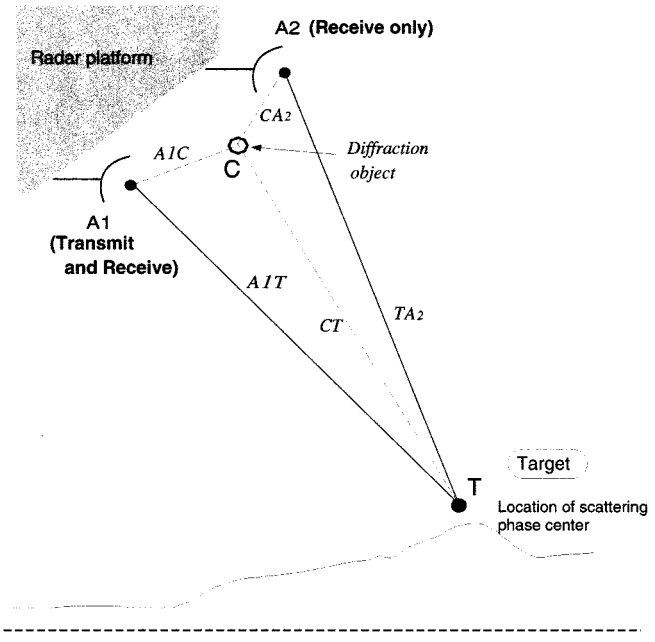

Fig. 6. Multipath problem.

height. Such a model has been developed using fractal-generated trees by Lin and Sarabandi [14], [15].

Using cylinders, disks, and needles, a full-wave Monte Carlo simulation was used to estimate powers and scattering

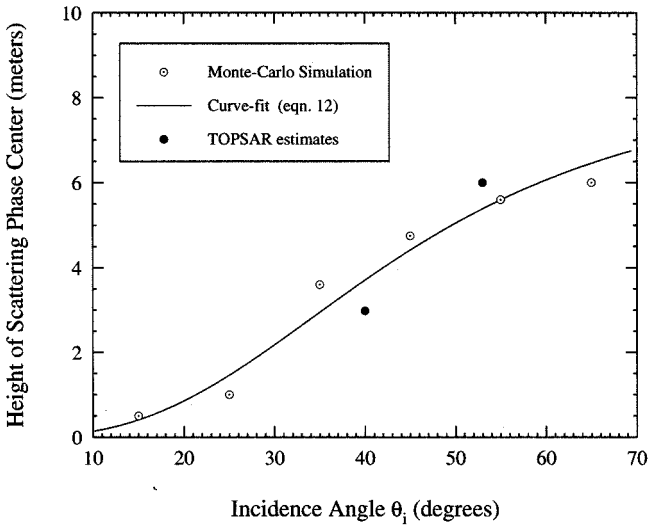

Fig. 7. Estimated height of the scattering phase center of Stand 22 compared with the height extracted from the two TOPSAR images of the same stand. This figure is adapted from a similar figure in [12].

phase center heights for several different tree stands at several incidence angles. The major lessons are that the height of the scattering phase center varies with incidence angle and with the extinction distribution in the tree canopy. Typically, the height was higher for large incidence angles and for large total extinctions. However, the calculated phase center height never achieved the true tree height, and often was significantly less, down to one-tenth or less of the true height. This means that some kind of model must be used in order to obtain tree heights from a TOPSAR DEM, even after we estimate the phase center height.

A heuristic model for tree height of red pine stands given the phase center height, incidence angle, and extinction [or correlation] is now developed. Fig. 7 shows the results for the fractal model described above as applied to one stand at the MFTS. Recall that the tree stands chosen for this study were monocultures all planted at the same time, resulting in a very uniform height distribution. The sigmoidal shape can be modeled with

$$h_{ph} = h_o \frac{(\theta/\theta_o)^n}{1+(\theta/\theta_o)^n} \tag{12}$$

where

h_{ph}	phase center height;
h_o	true height;
θ	incidence angle;
θ_o	free parameter that corresponds to the incidence angle where the curve has an inflection point;
power n	free parameter, but could depend on extinction, with higher n corresponding to higher extinction.

The best-fit curve to the C_{vv} data is also shown in Fig. 7. For that data, a simple least-squares fit gives $n = 2.7$ and $\theta_o = 45°$. As a first approximation, for all the other data in this study we will assume that only h_o changes. This gives us a family of curves that we can use to easily estimate h_o given h_{ph} and θ. This is crude and probably only works for red pine trees at this test site, but further refinements must await more simulations with the fractal model.

TABLE IV
RESULTS OF EXTRACTED TREE HEIGHT FROM TOPSAR DEM. HEIGHT EXTRACTED BY METHOD 2 FITS IN THE TREND THAT THE HEIGHT OF SCATTERING PHASE CENTER WILL INCREASE AS THE INCIDENCE ANGLE INCREASES AND IT ALWAYS APPEARS BELOW THE CANOPY TOP, WHEREAS HEIGHT EXTRACTED BY METHOD 1 DOESN'T ALWAYS FIT THIS TREND

(a) Extracted by using DGPS data. (Method (1))

Stand No.	phase center height (CCTID:TS0149) [meters]	phase center height (CCTID:TS0171) [meters]	Modeled Tree ht [meters]	Actual tree height [meters]
22 (incidence angle)	3.8 (40°)	7.0 (53°)	9.0, 11.4	8.7
68 (incidence angle)	8.0 (49°)	5.5 (59°)	14.2, 8.0	13.8

(b) Extracted by using elevation difference between the forest stand and the nearby flat area. (Method (2))

Stand No.	phase center height (CCTID:TS0149) [meters]	phase center height (CCTID:TS0171) [meters]	Modeled Tree ht [meters]	Actual tree height [meters]
22 (incidence angle)	3.0 (40°)	6.0 (53°)	7.0, 9.7	8.7
68 (incidence angle)	7.7 (49°)	9.0 (59°)	13.6, 13.1	13.8

Remark:
1) Source of actual tree height and species are from [2].

There are two ways of determining the height of the scattering phase center h_{ph} for use in height estimation. First, if the TOPSAR DEM is correct in an absolute sense, then a simple subtraction of the known DEM of the area from the USGS data is sufficient. However, as seen previously, generating correct TOPSAR DEM data is laborious. An alternative is to use the good relative heights. In this scheme, there must be a bare and flat area near the tree stand of interest in order to be able to have confidence that the subtraction gives meaningful results. Since we were able to find appropriate areas in the images, we used both methods. Table IV shows the results of the phase center height estimation and the tree height estimation for several stands. Only two stands were used for several reasons.

1) We were limited to monoculture pine stands so thta we could use the model.
2) The stand must appear in both TOPSAR images in order to have data for two different incidence angles.
3) An adjacent bare, flat surface at the same range for subtraction within the DEM, while avoiding multipath errors.

For each tree stand, we used the GPS data for the subtraction as well as the TOPSAR DEM. As you can see, both methods yield similar results that compare well with the ground-based measurements of the tree height. The comparison with any independently measured elevation still suffers due to the residual multipath errors, with an error as high as 2.65 m or 30% for stand 22. The worst-case error when using a nearby flat area for reference is 1 m or 11%. It is hoped that removal of the multipath errors will allow comparison with ground-based measurements to yield accurate tree height estimations.

IV. CONCLUSIONS

While the data from the TOPSAR has problems with roll angle errors and multipath, it appears that these can either be fixed or judiciously avoided. A nicer method to deal with the roll angle error would not require a known DEM.

Tree height determination seems feasible, but we need more sophisticated models in order for it to work for a greater variety of trees. This work is in progress.

Another method of tree height determination could use more frequencies and polarizations so that a reference height is unneeded.

ACKNOWLEDGMENT

The authors wish to thank the JPL Radar Science group for their help in providing the TOPSAR image data used in this study and especially Dr. Y. Kim for corresponding with us regarding this study.

REFERENCES

[1] J. I. H. Askne, P. B. G. Dammert, L. M. H. Ulander, and G. Smith, "C-band repeat-pass interferometric SAR observations of the forest," *IEEE Trans. Geosci. Remote Sensing*, vol. 35, pp. 25–35, Jan. 1997.
[2] K. M. Bergen, M. C. Dobson, T. L. Sharik, and I. Brodie, Tech. Rep. 026 511-7-T, "Structure, Composition, and Above-ground Biomass of SIR-C/X-SAR and ERS-1 Forest Test Stands 1991-1994, Raco Michigan Site," University of Michigan, Ann Arbor, Oct. 1995.
[3] S. R. Cloude and K. P. Papathanassiou, "Polarimetric SAR interferometry," *IEEE Trans. Geosci. Remote Sensing,*, vol. 36, pp. 1551–1565, Sept. 1998.
[4] M. C. Dobson, F. T. Ulaby, and L. Pierce, "Land-cover classification and estimation of terrain attributes using synthetic aperture radara," *Remote Sens. Environ.*, vol. 51, pp. 199–214, Jan. 1995.
[5] M. C. Dobson, F. T. Ulaby, L. Pierce, T. L. Sharik, K. M. Bergen, J. M. Kellndorfer, J. R. Kendra, E. Li, Y.-C. Lin, A. Nashashibi, K. Sarabandi, and P. Siqueira, "Estimation of forest biophysical characteristics in Northern Michigan with SIR-C/X-SAR," *IEEE Trans. Geosci. Remote Sensing*, vol. 33, pp. 877–895, July 1995.
[6] M. C. Dobson, L. E. Pierce, and F. T. Ulaby, "Knowledge-based land-cover classification using ERS-1/JERS-1 SAR composites," *IEEE Trans. Geosci. Remote Sensing*, vol. 33, pp. 83–99, Jan. 1996.
[7] J. O. Hagberg, L. M. H. Ulander, and J. I. H. Askne, "Repeat-pass SAR interferometry over forested terrain," *IEEE Trans. Geosci. Remote Sensing*, vol. 33, pp. 331–340, Mar. 1995.
[8] L. E. Pierce, F. T. Ulaby, K. Sarabandi, and M. C. Dobson, "Knowledge-based classification of polarimetric SAR images," *IEEE Trans. Geosci. Remote Sensing*, vol. 32, pp. 1081–1086, Sept. 1994.

[9] G. Schreier, Ed., *SAR Geocoding: Data and Systems*. Berlin, Germany: Wichmann, 1993.
[10] H. A. Zebker, S. N. Madsen, J. Martin, K. B. Wheeler, T. Miller, Y. Lou, G. Alberti, S. Vetralls, and A. Cucci, "The TOPSAR interferometric radar topographic mapping instrument," *IEEE Trans. Geosci. Remote Sensing*, vol. 30, pp. 933–940, May 1992.
[11] S. N. Madsen, H. A. Zebker, and J. Martin, "Topographic mapping using radar interferometry: Processing techniques," *IEEE Trans. Geosci. Remote Sensing*, vol. 31, pp. 246–256, Mar. 1993.
[12] S. N. Madsen and H. A. Zebker, "Automated absolute phase retrieval in across-track interferometry," in *IGARSS'92: Proc. 1992 Int. Geoscience and Remote Sensing Symp.*, vol. 2, Houston, TX.
[13] Y. J. Kim, , personal communication.
[14] Y. C. Lin and K. A. Sarabandi, "Monte Carlo coherent scattering model for forest canopies using fractal generated trees," *IEEE Trans. Geosci. Remote Sensing*, vol. 37, pp. 440–451, Jan. 1998.
[15] K. Sarabandi and Y. C Lin, "Simulation of interferometric SAR response for characterizing the scattering phase center statistics of forest canopies," *IEEE Trans. Geosci. Remote Sensing*, vol. 35, pp. 115–125, Jan. 1997.
[16] Y. Kim *et al.*, "NASA/JPL airborne three-frequency polarimetric/interferometric SAR system," in *1996 Int. Geoscience and Remote Sensing Symp.*, pp. 1612–1614.
[17] R. N. Treuhaft, S. N. Madsen, M. Moghaddam, and J. J. van Zyl, "Inteferometric remote sensing of vegetation and surface topography," *Radio Sci.*, vol. 31, pp. 1449–1485.
[18] K. Sarabandi, "$\triangle k$-radar equivalent of interferometric SARs: A theoretical study for determination of vegetation height," *IEEE Trans. Geosci. Remote Sensing*, vol. 35, pp. 1267–1276, Sept. 1997.

Yutaka Kobayashi received the B.S. and M.S. degrees in electrical engineering from the University of Tokyo, Japan, in 1988 and 1990, respectively.

Since 1990, he has been working for Toshiba, Tokyo, Japan, as a Radar System Engineer. From 1996 to 1997, he was with the Radiation Laboratory, Department of Electrical Engineering and Computer Science, University of Michigan, Ann Arbor, as a Visiting Scholar carrying out the study of interferometric SAR (INSAR), described in this paper. His research interests include radar system design and signal processing of INSAR.

Kamal Sarabandi (S'87–M'90–SM'92–F'00) received the B.S. degree in electrical engineering from Sharif University of Technology, Tehran, Iran, in 1980, and the M.S.E. degree in electrical engineering and the M.S. degree in mathematics and the Ph.D. degree in electrical engineering, all from the University of Michigan, Ann Arbor, in 1986 and 1989, respectively.

From 1980 to 1984, he worked as a Microwave Engineer with the Telecommunication Research Center, University of Michigan, where he is currently the Director of the Radiation Laboratory and an Associate Professor with the Department of Electrical Engineering and Computer Science. He has 18 years experience with microwave sensors and radar systems. In the past eight years, he has served as Principal Investigator and Co-Investigator on many projects sponsored by NASA, JPL, ARO, ONR, ARL, NSF, and numerous industries. He has published many book chapters and more than 85 papers in refereed journals on electromagnetic scattering, random media modeling, wave propagation, microwave measurement techniques, radar calibration, application of neural networks in inverse scattering problems, and microwave sensors. He has also had more than 160 papers and invited presentations in national and international conferences and symposia on similar subjects.

Dr. Sarabandi is listed in *American Men and Women of Science* and *Who's Who in Electromagnetics*. He has been a member of the IEEE Geoscience and Remote Sensing ADCOM since January 1998 and has served as the Chairman of Geoscience and Remote Sensing Society, Southeastern Michigan chapter from 1992 to 1998. He is also a member of Commission F of the URSI and the Electromagnetic Academy. He was a recipient of a 1996 Teaching Excellence Award, the 1997 Henry Russel Award from the Regent of The University of Michigan, and the 1999 GAAC Distinguished Lecturer Award from the German Federal Ministry for Education, Science, and Technology.

Leland Pierce (S'85–M'85–M'89) received the B.S. degree in both electrical and aerospace engineering in 1983, and the M.S. and Ph.D. degrees in electrical engineering in 1986 and 1991, respectively, all from the University of Michigan, Ann Arbor.

He is currently Head of the newly formed Microwave Image Processing Facility, Radiation Laboratory, Electrical Engineering and Computer Science Department, University of Michigan, Ann Arbor, where he is responsible for research into the uses of Polarimetric SAR systems for remote sensing applications, specifically, forest canopy parameter inversion.

M. Craig Dobson received the B.A. degree in geology and anthropology from the University of Pennsylvania, Philadelphia, PA, in 1973, and the M.A. in geography from the University of Kansas, Lawrence, in 1981.

He has been a Member of Research Faculty, Radiation Laboratory, University of Michigan, Ann Arbor, since 1984 and was previously with the Center for Research, University of Kansas, Lawrenceville. His interests include basic and applied research in the field of microwave remote sensing. His prior work ranges from measurement and modeling of the fundamental microwave dielectric properties of natural terrestrial media (soil, vegetation, and snow) to measurement and modeling of the microwave emission and radar backscattering from terrain. His past research conducted at the laboratory and plot scale have led to applied research in the areas of remote sensing of near-surface soil moisture, land-cover classification, and the retrieval of biophysical estimates of attributes such as vegetation height, basal area, above ground biomass, timber volume, and carbon storage. This work has been extended to simulation of the expected performance of the next generation of orbital SAR systems now being designed and constructed by Japan, Canada, Europe, and the U.S. He is currently engaged in large-scale assessment of tropical forests using archival SAR data and joint projects with the US Forest Serve and timber companies to evaluate the use of SAR for forest assessment and management. Much of his research has been done in close collaboration with ecologists, soil scientists, and hydrologists in an interdisciplinary setting. He has written two books and several book chapters, authored 47 journal publications, and presented 156 papers at technical symposia.